Rolling SLIP Model Based Running on a Hexapod Robot

Chun-Kai Huang, Ke-Jung Huang, and Pei-Chun Lin

Abstract—We report on development of dynamic running behavior on the RHex-style hexapod robot. By using the Rolling SLIP (R-SLIP) model as the "template" of the robot, together with the investigation of the stability properties of the R-SLIP model, the robot implemented with the selected trajectory based on the R-SLIP motion can immediately excite its dynamic running behavior (i.e., composed of stance and flight phases) without necessity of extra tuning or optimization effort. In addition, a feedback control strategy is proposed to regulate the robot's motion when the robot's operating region is not located at the stable area of the R-SLIP model (i.e., no stable fixed point). The controller includes three portions: a body velocity estimator, a database containing a wide range of pre-computed R-SLIP trajectories, and a control law which regulates the robot motion to the desired R-SLIP profile. The proposed methodology of robot trajectory generation and strategy of running regulation are experimentally evaluated.

I. INTRODUCTION

The study of the robot system dynamics was first investigated on the monopods in the 80s [1]. After the initiation, various legged robots were designed for dynamic locomotion, including quadruped robots [2-4] and hexapod robots [5-7]. Dynamic locomotion of the legged robots is mainly inspired by that of the legged animals, which can be approximated by a spring loaded inverted pendulum (SLIP) [8-10], no matter how complex the morphology of the original creatures are. Owing to the intrinsic characteristics of the SLIP itself as well as the empirical difficulty of implementing this model to the real robots, recently many new forms of the dynamic models are developed, for example, a SLIP model with a half-circle foot [11, 12], a two-segmented leg model with a torsional spring in between [13], a rolling-SLIP (R-SLIP) model which has a torsional spring and a large scale rolling surface [14], a clock-torque SLIP model [15], torque-actuated SLIP model [16], and etc. However, most of the reported works are still constrained in the model analysis and not yet linked to the robot operation. On the other hand, the majority of developed dynamic robots focus on the careful design of the robot platform which allows the robot to excite dynamic behaviors via simple open-loop strategy, or focus on understanding the dynamic models of the designed robots. Not much work addresses the issue how to excite the SLIP-like running behavior on the given robot from the aspect of trajectory design and control.

Here, we report on our investigation of developing a strategy which allows us to excite the robot dynamic locomotion based on the intrinsic, reduced-ordered, dynamic
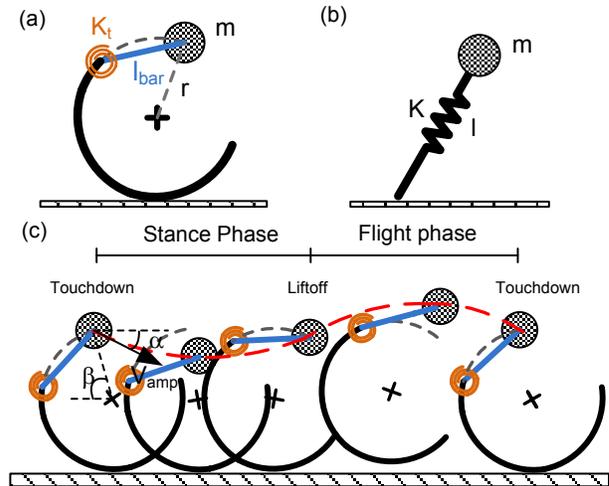
Fig. 1. Characteristics of the R-SLIP model: (a) Intrinsic parameters of the R-SLIP model; (b) instrinsic parameters of the traditional SLIP model; (c) ilustrative sketch of the running motion of the R-SLIP mdoel with stance phase and flight phase.

SLIP-based model. Instead of using the traditional SLIP model, the R-SLIP model [14] was utilized as the "template" [17] of the robot because of the rolling and stiffness-changing characteristics of the half-circle legs on the robot during its locomotion. Having R-SLIP as the control guidance, we firstly investigate its stability property and find the adequate region which is empirically achievable by the robot platform. To further regulate the dynamic running motion, a control strategy is also proposed which includes three essential components: a body velocity estimator, a database filling with a wide range of usable R-SLIP trajectories, and a controller which regulate the dynamic motion of the robot to the nominal settings. The proposed strategy is implemented on the RHex-style robot and experimentally evaluated.

The rest of this paper is organized as follows. Section II briefly reviews the R-SLIP model. Section III describes the stability region of the R-SLIP model which can be adopted by the physical robot. Section IV demonstrates trajectory generation and control strategy. Section V reports the results of experimental evaluation, followed by conclusion in Section VI.

II. BRIEF REVIEW OF THE R-SLIP MODEL

The previously-developed R-SLIP model [14] shown in Fig. 1(a) is utilized as the control template to regulate the dynamic motion of the robot. Instead of using the ordinary SLIP model shown in Fig. 1(b), utilization of the R-SLIP model is merely judged by the dynamic behavior of the experimental platform, where the dynamic characteristics of the "virtual leg" in the R-SLIP model fits better with the empirical compliant circular legs on the RHex-style robot

than the ordinary SLIP model does. Note that the methodology proposed in this work is indeed independent to the platform and it can be deployed to other legged robots as long as the "template" of the robot is defined [17].

The basic characteristic of the R-SLIP model is described as follows. It has two rigid segments, a bar and a circular rim, connected by a torsional spring. The other end of the bar has a point mass, and the circular rim contacts with the ground as shown in Fig. 1(a). Therefore, the R-SLIP has four intrinsic parameters: mass (m), stiffness of the torsional spring (K_t), radius of the circular rim (r), and the distance between the torsion spring and the mass (l_{bar}). In contrast, the ordinary SLIP model only has three intrinsic parameters: mass (m), stiffness of the spring (k), and length of the spring (l). Figure 1(c) shows a full stride of the R-SLIP model in its running motion, which has stance phase and flight phase, alternating periodically with each other. The initial conditions at each landing are landing angle (β), touchdown speed (v_{amp}), and touchdown angle (α) which is included by the touchdown velocity and the horizontal line. The first condition indicates how the leg poses when the R-SLIP touches the ground, and the latter two conditions represent the magnitude and angle of the initial velocity of the R-SLIP mass. With given initial conditions and model parameters, a complete motion sequence of the R-SLIP model can be derived and simulated.

III. STABILITY ANALYSIS OF THE R-SLIP MODEL

It is important to investigate the adequate running conditions of the R-SLIP model itself, so when it is served as the template of the running robot, the intrinsic stability characteristics would help the robot to be operated in the natural dynamic region with minimum control effort. Following our dimensionless steps-to-fall and return-map analysis for stability investigation reported in [14], here we rerun these works and focused on the parameter range which matches the physical characteristics of the experimental platform, to make sure the selected R-SLIP behavior can be empirically excited on the RHex-style robot. Because the intrinsic parameters of the model (m, K_t, r, l_{bar}) are completely dependent on the robot's physical properties and are not adjustable ($r = 0.0725m$, $K_t = 7.6N/m$, $m= 6.266/3=2.089Kg$, $l_{bar} = 0.079m$), the analysis is focused on varying the initial conditions (I.C.s): touchdown velocity (v_{amp}, α) and landing angle (β).

The steps-to-fall analysis examines ability of the R-SLIP model to periodically keep its stable running behavior without falling down. Similar to the method reported in [13, 18], it simply counts the successive steps, and the threshold is set as 25 strides. The falling-down conditions is either (i) the lift-off velocity is in the backward direction and (ii) the body doesn't lift-off at all and hits the ground. Figure 2 shows the results of the steps-to-fall analysis of the R-SLIP model. Four different landing speeds are investigated (v_{amp}=1, 1.25, 1.5, and 1.75m/s), which are determined by the achievable motor speeds on the RHex-style robot. With each landing speed the other two parameters, α and β, are varied to search for the operatable region. The plots reveal several characteristics: (i) area of the stable region increases when the touchdown speed
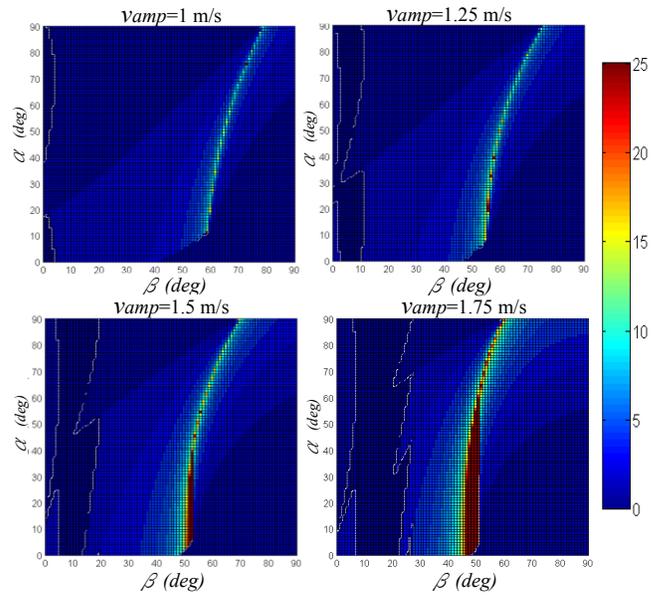
Fig. 2. Steps-to-fall analysis of the R-SLIP model: The regions with different colors indicate how many strides the R-SLIP can perform before it falls down. The vertical bar on the right side reveals relation between the color and the numbers of strides.
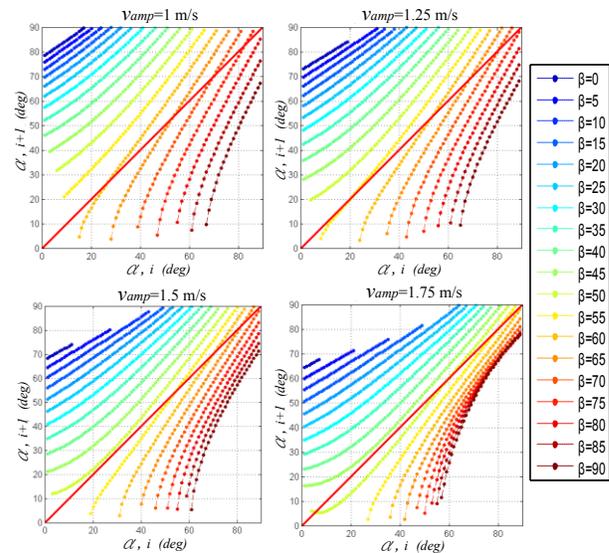
Fig.3. Return map analysis of the R-SLIP model.

(v_{amp}) increases. The touchdown speed can further be regarded as the energy level in the system. (ii) The adequate range of the touchdown angle (α) falls within 5 to 20deg. Taking v_{amp} equal to 1.25m/s as an example, the touchdown angle is around 20deg for stable motion. (iii) The landing angle (β) of the R-SLIP has a lower limit for stable motion, and this phenomenon is similar to the two-segment legged model reported in [13]. In addition, the minimum landing angle (β) for stable motion decreases while the touchdown speed increases. For instance, the values are around 56deg and 47 deg while the touchdown speeds are 1.25m/s and 1.75m/s, respectively.

Steps-to-fall analysis provides an overview that roughly points out the adequate ranges of parameters for stable running motion. However, it cannot qualitatively predict the R-SLIP behavior even if the parameter set can let the R-SLIP

successfully run *25* steps. Return map of the parameter touchdown angle (α) is utilized to check the condition of fixed points of the system. In this single-step analysis, the stability is judged by the relationship of touchdown velocity between current the ith touchdown and the next $i+1^{th}$ touchdown, and the fixed point exists while the next touchdown angle is the same as that at current touchdown. Moreover, the fixed point can potentially be self-stable in a limit cycle if its derivative satisfies the slope condition. Figure 3 shows the results of the return map analysis of the R-SLIP model. The range of touchdown speed is set the same as those in steps-to-fall analysis: v_{amp}=*1, 1.25, 1.5,* and *1.75m/s*. In each plot, curves with different colors represent the model with different landing angles (β). The fixed points appear when the landing angle is around *50* to *60deg*. Both the range and the stability characteristics (i.e., determined by the slope of the fixed point) increases when the touchdown speed (i.e., system energy) increases. The results are consistent with those shown in the steps-to-fall analysis.

IV. Strategy of Robot Running Motion Regulation

The results described in the previous section shows the range of adequate initial conditions where the R-SLIP model would perform stable running motion. By importing this specific trajectory into the robot, ideally the robot should be able to move as planned (hereafter referred to as "open-loop" method). Empirically we found that the robot implemented with this trajectory can indeed excite its dynamic behavior (i.e., running with aerial phase) without any tuning or trajectory modification effort. However, owing to imperfect experimental and environmental setting, the robot usually exhibit motion in a more complex manner. For example, the three legs in the same tripod may not touch and leave the ground simultaneously, and this behavior further causes unwanted pitch and roll motion of the robot. When the initial conditions of the robot in a specific stance phase are not the same as planned ones, if a pre-planned leg trajectory with that specific I.C. is still forced to deploy on the robot, the original robot dynamics is actually disturbed in a worse manner. In this case, the running motion of the robot is excited unregularly, resulting in non-stable running motion.

To remedy the discrepancy between the ideal single-leg R-SLIP model and the empirical hexapod with two tripods, a strategy for running motion regulation should be deployed on the robot. Adjusting the pitch and roll motion of the robot in general require state and/or force information of all legs, and the adjustment may also break the original tripod configuration, which makes the excitation of running more complicated. Therefore, in our approach we tried to keep the tripod configuration unaltered. Instead, the regulation strategy focuses on how to deploy an adequate trajectory to the tripod at every stance phase with given I.C.s. The R-SLIP model can perform different running behaviors with different I.C.s if the operation region falls in an adequate and stable region. Thus, when the robot lands the ground with a specific I.C., a specific trajectory for the robot can be found which preserves the natural dynamics of the R-SLIP model. Even

though at this specific stride the R-SLIP trajectory is not the same as that in the previous stride, the running motion of the robot can at least be preserved. However, the strategy so far may not be sufficient for stable running because in this case the disturbance would act as the main driving force to affect the I.C. of the next stride, and the running motion may diverge and gradually move to the unstable running region. Therefore, a regulation should be deployed to make sure that the running motion in the next stride is toward the desired running trajectory.

The proposed running motion regulation system is composed of several sub-systems: (i) a touchdown condition estimator, where the I.C. of each stride on the stance phase can be yielded. (ii) A database which contains a wide range of CoM trajectories, each correspond to a specific I.C. (iii) A trajectory selector, which finds the suitable CoM trajectory with a specific and given I.C. Thus, when the robot touches the ground with a specific I.C., this I.C. is estimated by the estimator, and then the trajectory selector yields a suitable trajectory for the next stride, which will gradually pull the trajectory back to the nominal pre-planned trajectory. The sub-systems are described separately as follows:

A. Design of the touchdown condition estimator

As mentioned in Section II, the R-SLIP model has three initial conditions: landing angle (β), touchdown speed (v_{amp}), and touchdown angle (α). The analysis in Section III shows that for given proper v_{amp} and α, a fixed point can be found. This phenomenon implies that if v_{amp} and α are known, a specific trajectory can be defined which has the stable running property. Thus, a touchdown condition estimator is designed to estimate the touchdown velocity, including its magnitude (v_{amp}) and angle (α).

The touchdown estimator relies on the sensory information from both inertial measurement unit (IMU) and joint encoders. The IMU can catch the dynamics of the locomotion, but it also suffers the drifting phenomenon which severely deteriorates the trustable level of the information. Thus, the joint encoders are incorporated to reduce the drifting error. First, the instantaneous forward and vertical velocities are derived by integration of the accelerations measured by accelerometers of the IMU, which runs continuously through the whole locomotion. In parallel, the velocities of the robot at its stance phase can also be estimated by the joint encoders. Because the former estimated velocities drifts gradually, the averaged velocities of the latter one is used to compensate the drifting behavior.

B. Generation of the database with various running trajectories with different initial conditions

Given a specific initial velocity (v_{amp} and α) located within the adequate range of stable running shown in Fig. 2 and Fig. 3, a search algorithm is designed to find the landing angle (β) which yields the stable running behavior (i.e, the fixed point). After the most adequate landing angle is found, the complete trajectory with this specific initial condition is defined, including both stance phase and ballistic flight phase. In
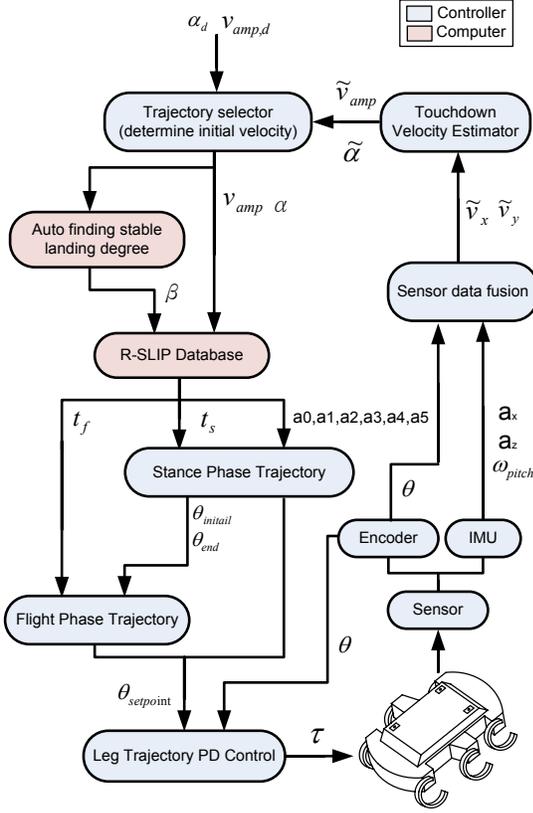
Fig. 4. Control strategy of the robot.

RHex information		
Body mass	M	6.266 kg
Body length	L	0.47 m
Body width	W	0.23 m
Body height	H	0.17 m
R-SLIP Model parameters		
Equivalent mass	m	2.089 kg
Leg radius	r	0.0725 m
Torsional spring position	ξ	66 degree
Leg torsional spring constant	Kt	7.6 N/m
Rigid bar length	lbar	0.079 m

addition, because the trajectory is located at the fixed point, the initial condition at next touch down is expected to be the same as the current one.

Because the dynamics of the R-SLIP is nonlinear, real-time trajectory generation takes significant amount of computation resource, and it is unfavorable for robot real-time operation. Thus, a database which includes the trajectories with a wide range of initial conditions is built offline and stored in the onboard memory on the robot. Instead of just storing the corresponding CoM trajectory to each initial condition, the offline computation also covers nonlinear inverse kinematics, and the derived joint angle versus time is further approximated by a fifth-order polynomial (i.e., six coefficients). More specifically, the CoM trajectory of the R-SLIP model is stored in the form of polynomial function. Together with two additional information, time for the stance phase time (t_s) and that for the flight phase time (t_f), the data for each initial condition set has 8 scalar components. The six coefficients and the time for the stance phase are sufficient to generate correspond joint trajectory of the robot in stance phase. By using the initial and final positions of the stance phase and the time for flight phase, the ballistic flight trajectory can be found. In the empirical application the flight trajectory is not critical, this time period is used to pose the leg in the right configuration for the next touchdown. In order to make the trajectory has smooth transition between stance and flight phases, a smooth function is added.

The database covers the initial conditions with touchdown speed (v_{amp}) from 0.7 to 2.1 m/s and touchdown angle (α)

from 10 to 40 degrees. The lower bound is defined based on the stability analysis described in Section III, and the upper bound is constraint by the motor speed limit.

C. Trajectory selector

In order to gradually move the running trajectory to the desired profile, the actual joint trajectory applied to the next stance phase will not be the one matched the estimated touchdown condition $(\widetilde{v}_{amp}, \widetilde{\alpha})$, but the one with modified initial condition, (v_{amp}, α), which located between the current and the desired initial conditions, $(v_{amp,d}, \alpha_d)$. The formula is

$$v_{amp} = sat[v_{amp,d} + k_1(v_{amp,d} - \widetilde{v}_{amp})],$$
$$\alpha = sat[\alpha_d + k_2(\alpha_d - \widetilde{\alpha})] \tag{1}$$

where the parameters k_1 and k_2 are set to 0.6 and 0.2 based on performance of the empirical robot. The function $sat[]$ represents the saturation function, which is bounded by the range of the initial conditions provided in the database.

In summary, the flow chart of the overall regulation strategy is depicted in Fig. 4.

V. EXPERIMENT EVALUATION

The RHex-style robot shown in Fig. 5(a) was utilized for experimental evaluation of the proposed algorithm. The robot has a real-time embedded control system (sbRIO-9602, National Instruments) running at 500Hz. The onboard IMU is comprised of one 3-axis accelerometer (ADXL330, ±3g, Analog Device) and three 1-axis rate gyros (ADXRS610, ±3000/s, Analog Device). Table I lists physical parameters of RHex and the intrinsic parameters of R-SLIP model. The position and the stiffness of the torsional spring are determined by the same method as in [7].

Figure 5(b) shows the schematic map of the robot motion. Similar to the R-SLIP model, for each tripod of the robot, a full stride includes one stance phase and one aerial phase, where the state of the robot during locomotion can be roughly determined by time provided by the R-SLIP model. Because the robot runs with two tripods which alternate periodically, the period of the tripod is twice as that of the robot trajectory. Therefore, the aerial phase of the tripod contains two flight phases and one stance phase of the robot. Because in the algorithm the robot may use different R-SLIP models for each stride, for the continuity of the trajectory, the trajectory
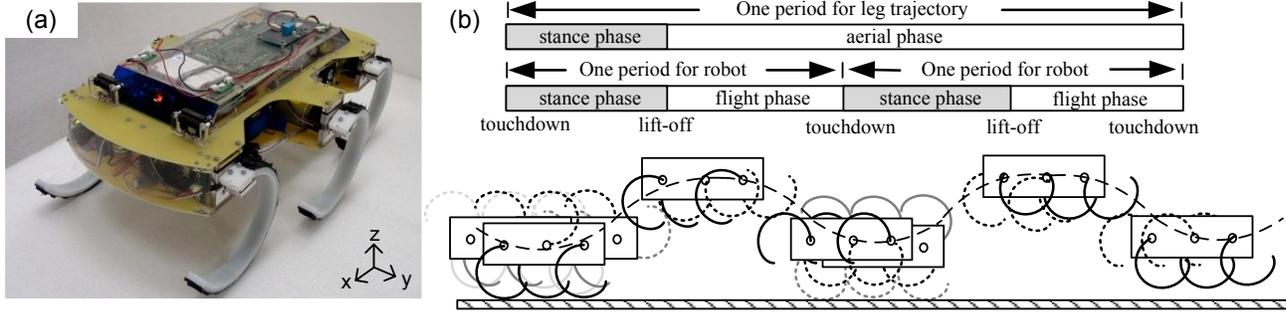
Fig. 5. (a) The RHex-style robot for experimental evaluation of the proposed strategy. (b) Dynamic running locomotion of the robot with two tripods.
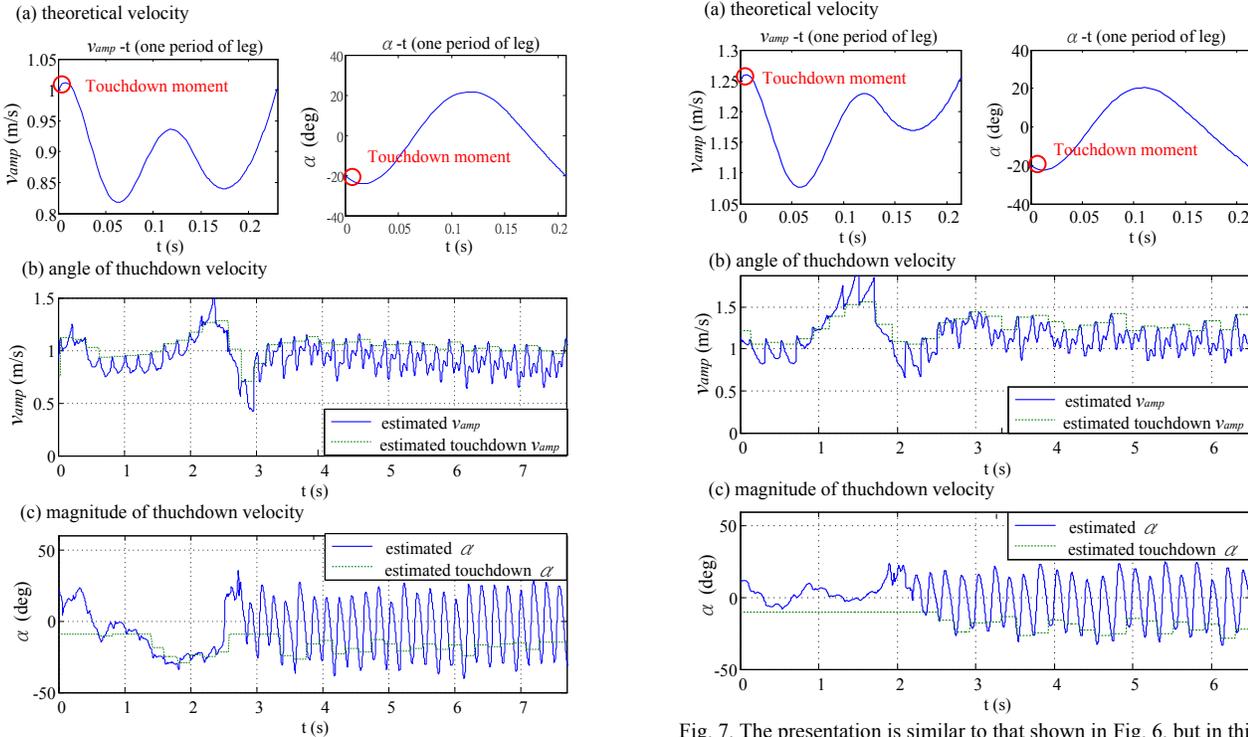
Fig. 6. Velocity of the robot estimated by the estimator, including magnitude (v_{mag}) and angle (v_{ang}) of the body velocity. The robot was set to run at touchdown speed: v_{amp}=1m/s and α=20deg. Subfigure (a) shows the theoretical velocity versus time of the R-SLIP model in one touchdown period, and subfigures (b) and (c) plot the magnitude and angle of the touchdown velocity, respectively.

switching is executed when the tripod is posed vertically toward the top direction. The RHex self-stabilized to the initial condition after being thrust down to the ground. According to the stability analysis described in Section III, the initial conditions for running motion on the robot was set as follow: α=20deg with v_{amp}= 1 and 1.25m/s, respectively. Ideally the magnitude of landing velocity should be higher; however, the achievable leg speed is now limited by the mechatronic system on the robot.

The performance of the feedback control strategy relies on accuracy of the estimated touchdown velocity; therefore, the performance of the touchdown condition estimator should be evaluated firstly. Figure 6 and 7 show results of the estimated velocity, each corresponding to one of the two nominal initial velocities. In this set of experiments the robot ran with nominal trajectory derived by the R-SLIP model without any control effort. Thus, the performance of the estimator can be

Fig. 7. The presentation is similar to that shown in Fig. 6, but in this figure the robot was set to run at touchdown speed: v_{amp}=1.25 m/s and α=20 deg.

roughly judge by the similarity of the state behavior of the model and the estimator. Subfigure (a) shows the theoretical velocity versus time in one touchdown period, and the subfigures (b) and (c) plot the magnitude and angle of the touchdown velocity, respectively. The blue solid curves represent the estimated velocity of the robot versus time, and the green dotted curves indicate the estimated touchdown velocity of the individual strides, which will be used as the indicator for the model selector to choose the suitable R-SLIP model of the next stride. Couple observations can be drawn from the information provided by this figure: First, with the nominal trajectory generated according to the R-SLIP model, even without feedback control strategy, the robot performs running locomotion with self-stabilized behaviors. The motion of the robot in the first two seconds is very irregular, but after that the robot is stabilized to the periodic motion. This phenomenon confirms that the R-SLIP model can indeed be regarded as the "template" of the robot. The behavior of the compliant half-circle leg can be approximated by a torsional spring with rolling contact. Second, both the timing

TABLE II THE EXPERIMENT RESULTS

$v_{amp,d}$=1 (m/s) ; $\alpha_{,d}$=20 (deg)				
	Open-loop		Closed-loop	
Exp. No.	$v_{amp,ave}$	$\alpha_{,ave}$	$v_{amp,ave}$	$\alpha_{,ave}$
1	1.03	16.15	1.04	18.91
2	1.05	16.27	1.04	19.33
3	1.05	19.59	1.03	18.85
4	1.03	15.18	1.03	17.38
5	1.04	16.75	1.02	16.20
6	1.07	22.13	1.01	17.79
Mean	1.05	17.68	1.03	18.08
Std	0.012	2.413	0.012	1.078
% Error	5.0%	-11.6%	3.0%	-9.6%
$v_{amp,d}$=1.25 (m/s) ; $\alpha_{,d}$ =20 (deg)				
	Open-loop		Closed-loop	
	$v_{amp,ave}$	$\alpha_{,ave}$	$v_{amp,ave}$	$\alpha_{,ave}$
1	1.30	19.87	1.30	19.66
2	1.33	21.70	1.28	19.48
3	1.28	20.83	1.34	20.07
4	1.32	19.27	1.32	22.14
5	1.31	20.52	1.27	21.72
6	1.28	20.43	1.25	20.70
Mean	1.30	20.44	1.29	20.63
Std	0.020	0.758	0.031	1.003
% Error	4.0%	2.2%	3.2%	3.2%

Fig. 8. Velovity of the robot measured by the GTMS, including magnitude (v_{amp}) and angle (v_{ang}) of the body velocity. The robot ran at two different speeds: v_{amp}=1 m/s in (a) and v_{amp}=1.25m/s in (b). In each velocity condition the robot ran with two control strategies: open-loop and closed-loop. Blue (solid) curve represents the experimental result of the robot measured by GTMS and the red (dotted) curve represents the theoretical trajectory in one period based on R-SLIP model.

of the touchdown moment and magnitude of the touchdown velocity can be well estimated. This is crucial for the feedback control. Third, the trend of the velocity trajectory of the estimator is similar to that of the R-SLIP model, which reveals that the estimator is reliable. Together with the second statement, the results imply and the robot does run under the R-SLIP model.

Table II lists the experiment results while the robot ran with only nominal trajectory (i.e., open-loop) and with the closed-loop control strategy described in Section IV (i.e, closed-loop). Six experimental runs were executed for each condition, and in each run the result is averaged from the estimated velocity of consecutive 20 strides after the robot stabilized its running motion. The percentage error indicates the error between the averaged experimental values to the nominal value. For the open-loop case, the results show that the robot could be self-stabilized to the motion close to the designed R-SLIP motion. The stability of the robot in the high-speed case (v_{amp}=1.25 m/s) is better than that in the low-speed case (v_{amp}=1 m/s), especially in touchdown angle (α). This phenomenon also matches the stability analysis shown in Section III. For the closed-loop case, by adding the controller, the stability of the robot in the low-speed case is improved, especially the touchdown angle (α), which confirms that the controller can help the system to be operated in the designed domain. The effect of the controller in high-speed case is not that obvious. Perhaps the intrinsic stability of the robot operated in high-speed condition is robust enough to endow good running motion.

Besides the results provided by the state estimator, several experiments were also executed in the ground truth measurement system (GTMS) to yield true body state. The GTMS is composed of two 500Hz high-speed cameras (A504k, Basler) and two 6-axis force plates (FP4060-07, Bertec). Figure 8 shows the robot velocity versus time while the robot was the given two different nominal touchdown velocities: v_{amp}=1 m/s in (a) and v_{amp}=1.25 m/s in (b). In each velocity condition the robot ran with two control strategies: open-loop and closed-loop. Blue curve represents the experimental result measured by GTMS and the red curve represent the theoretical trajectory based on R-SLIP model. Considering the touchdown angle (α), no matter in low-speed or high-speed case, the performance of the robot is very close to the theoretical trajectory. The touchdown speed (v_{amp}) has some variation but the trend is similar. An supplementary video is also included with this paper.

Figure 9 shows the vertical ground reaction force (f_z) versus time measured by the force plate on the runway. This figure shows that the robot has periodic change of stance and aerial phases. The theoretical time periods of the stance phase and flight phase based on the R-SLIP models are *0.1296s* and *0.0778 s* respectively, where the information is also shown in the figure. This figure reveals that first, in the sense of time the motion of the robot is approximately matched to the theoretical time. Second, the switching between two phases
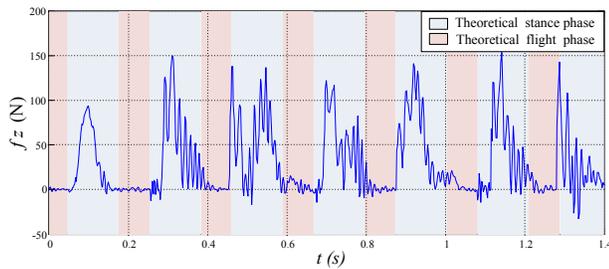
Fig. 9. The vertical ground reaction force (f_z) versus time of the robot measured by the GTMS. The colored background indicates the times of stance and flight phases the robot should perform based on the R-SLIP model.

Roll, mean	Roll, std	Pitch, mean	Pitch, std
-0.02 (deg)	2.06 (deg)	-0.15 (deg)	1.74 (deg)

locomotion stability in the low-speed case, but that in the high-speed case is not obvious and requires further investigation.

We are currently in the progress of remaking the whole robot to increase its mobility, so it can be operated in a more stable region of the R-SLIP model (i.e., at higher velocity). This allows us to investigate the balance of the intrinsic stable motion and the feedback effort.

on the robot is not so clear because the robot has two tripods and the three legs in each tripod may not touch or lift-off the ground simultaneously. Table III shows mean and standard deviation (std) of the roll and pitch angle of the robot, which are the averaged of all the experimental runs. The means are very close to zero, which indicates the tripod can be approximated by a single "virtual leg" in the current manner. If the mean is not close to zero, the three legs in the same tripod should move according to different trajectories. However, empirically the orientation of the robot indeed has some variations, where the stds of both states are around *2 degs*.

VI. CONCLUSION

We report on the development of the dynamic running behavior on the RHex-style hexapod robot. Instead of using the traditional SLIP model, the R-SLIP model was utilized as the "template" of the robot because of the rolling and stiffness-changing characteristics of the half-circle legs on the robot during its locomotion. The stability of the R-SLIP model within the achievable operating range of the robot is firstly investigated, including the analysis of steps-to-fall and return maps. Together with the mapping of the physical robot parameters to the R-SLIP model, the adequate operation conditions for the robot in the form of three initial conditions can be derived. The robot implemented with the selected two conditions (i.e., different velocities) can immediately excite its dynamic running behavior without necessity of extra tuning or optimization effort. The experimental results also confirm that the system stability can be improved if the system energy increases, which matches the results of stability analysis. To further improve the dynamic performance of the robot, a feedback control strategy is proposed to regulate the robot's motion. The controller includes three portions: (i) a body velocity estimator, which provides the estimation of the robot velocity, and the touchdown velocity is extracted for feedback; (ii) a database containing a wide range of pre-computed R-SLIP trajectories, which reduces the real-time computation load for deriving trajectory of the nonlinear R-SLIP model; (iii) A control law which regulates the robot motion to the desired R-SLIP profile. The proposed methodology and strategy are experimentally evaluated on the RHex-style robot within the GTMS. The results confirms that the self-stabilized property of the selected R-SLIP trajectory implemented on the robot, and the strategy of running regulation can improve the

REFERENCES

[1] M. H. Raibert, "Hopping in legged systems - modeling and simulation for the two-dimensional one-legged case," *IEEE Transactions on Systems Man and Cybernetics,* vol. 14, pp. 451-463, 1984.

[2] I. Poulakakis, J. A. Smith, and M. Buehler, "Modeling and experiments of untethered quadrupedal running with a bounding gait: The Scout II robot," *International Journal of Robotics Research,* vol. 24, pp. 239-256, Apr 2005.

[3] M. Buehler, R. Battaglia, A. Cocosco, G. Hawker, J. Sarkis, and K. Yamazaki, "SCOUT: A Ssmple quadruped that walks, climbs, and runs," presented at the IEEE International Conference on Robotics and Automation (ICRA), 1998.

[4] H. Kimura, Y. Fukuoka, and A. H. Cohen, "Adaptive dynamic walking of a quadruped robot on natural ground based on biological concepts," *International Journal of Robotics Research,* vol. 26, pp. 475-490, May 2007.

[5] U. Saranli, M. Buehler, and D. E. Koditschek, "RHex: A simple and highly mobile hexapod robot," *International Journal of Robotics Research,* vol. 20, pp. 616-631, Jul 2001.

[6] S. Kim, J. E. Clark, and M. R. Cutkosky, "iSprawl: Design and tuning for high-speed autonomous open-loop running," *International Journal of Robotics Research,* vol. 25, pp. 903-912, Sep 2006.

[7] K.-J. Huang, S.-C. Chen, and P.-C. Lin, "A Bio-inspired single-motor-driven hexapod robot with dynamical gaits," in *IEEE/ASME International Conference on Advanced Intelligent Mechatronics (AIM),* 2012.

[8] R. M. Alexander, *Elastic mechanisms in animal movement* Cambridge University Press 1988.

[9] M. H. Dickinson, C. T. Farley, R. J. Full, M. A. R. Koehl, R. Kram, and S. Lehman, "How Animals Move: An Integrative View," *Science,* vol. 288, pp. 100-106, April 7, 2000 2000.

[10] P. Holmes, R. J. Full, D. Koditschek, and J. Guckenheimer, "The dynamics of legged locomotion: Models, analyses, and challenges," *Siam Review,* vol. 48, pp. 207-304, Jun 2006.

[11] J. Y. Jun and J. E. Clark, "Effect of rolling on running performance," in *IEEE International Conference on Robotics and Automation (ICRA),* 2011, pp. 2009-2014.

[12] J. Y. Jun and J. E. Clark, "A reduced-order dynamical model for running with curved legs," in *IEEE International Conference on Robotics and Automation (ICRA),* 2012, pp. 2351-2357.

[13] J. Rummel and A. Seyfarth, "Stable running with segmented legs," *International Journal of Robotics Research,* vol. 27, pp. 919-934, Aug 2008.

[14] K.-J. Huang and P.-C. Lin, "Rolling SLIP: A model for running locomotion with rolling contact," in *2012 IEEE/ASME International Conference on Advanced Intelligent Mechatronics (AIM),* 2012, pp. 21-26.

[15] J. Seipel and P. Holmes, "A simple model for clock-actuated legged locomotion," *Regular & Chaotic Dynamics,* vol. 12, pp. 502-520, Oct 2007.

[16] M. M. Ankarali and U. Saranli, "Stride-to-stride energy regulation for robust self-stability of a torque-actuated dissipative spring-mass hopper," *Chaos,* vol. 20, Sep 2010.

[17] R. J. Full and D. E. Koditschek, "Templates and anchors: Neuromechanical hypotheses of legged locomotion on land," *Journal of Experimental Biology,* vol. 202, pp. 3325-3332, Dec 1999.

[18] A. Seyfarth, H. Geyer, M. Gunther, and R. Blickhan, "A movement criterion for running," *Journal of Biomechanics,* vol. 35, pp. 649-655, May 2002.